# *Kagomé* spin-$\frac{1}{2}$ antiferromagnets in the hyperbolic plane

Veit Elser and Chen Zeng
*Laboratory of Atomic and Solid State Physics, Cornell University, Ithaca, New York 14853-2501*
(Received 16 October 1992; revised manuscript received 23 November 1992)

Spin-dimerized states are useful in the construction of spin-disordered wave functions but difficult to deal with because of nonorthogonality. For the spin-$\frac{1}{2}$ *kagomé* antiferromagnet, a systematic expansion of matrix elements of these nonorthogonal states is made possible by considering generalizations of the *kagomé* structure in the hyperbolic plane. The first nontrivial term in this expansion is an effective spin Hamiltonian which describes resonance among dimerized states. Minimum-energy states of the effective Hamiltonian correspond to a high degree of resonance among a small fraction of the dimers.

## I. INTRODUCTION

Recent theoretical interest in the two-dimensional Heisenberg antiferromagnet with spins arranged in the *kagomé* structure was kindled by two unrelated experimental systems: (a) *kagomé* sheets of spin-$\frac{3}{2}$ $Cr^{3+}$ ions in the layered oxide $SrCr_{8-x}Ga_{4+x}O_{19}$ (Ref. 1), (b) nuclear-spin-$\frac{1}{2}$ moments of second-layer $^3$He atoms adsorbed on graphite.[2,3] While neither system is an ideal realization of the simple theoretical model, interest in the *kagomé* antiferromagnet has grown rapidly because of its unusual ordering properties. At high spin, calculations by Sachdev[4] and Chubukov[5] predict coplanar ordering of moments into the $\sqrt{3}\times\sqrt{3}$ pattern. For spin-$\frac{1}{2}$, however, there is strong numerical evidence that the average moment at each site vanishes. Singh and Huse[6] have performed a high-order perturbation expansion about the Ising limit of the Hamiltonian which corresponds to the $\sqrt{3}\times\sqrt{3}$ magnetically ordered state. The radius of convergence of the expansion was found to be well below the isotropic Heisenberg point, thus implying a new type of ordering in the isotropic model. Numerical diagonalization studies on a 36-site *kagomé* cluster[7] indicate a very rapid decay of the two-spin-correlation function in the ground state—again implying a new "exotic" type of ordering. Other two-dimensional quantum spin models with proven or proposed exotic ground states are considerably more contrived than the spin-$\frac{1}{2}$ *kagomé* system.

A popular strategy for exploring new phases of quantum antiferromagnets has been the use of $1/N$ expansions where $N$ represents the size of a suitable enlargement of the group SU(2). As emphasized by Sachdev,[4] expansion schemes differ not just in the choice of group but also in the choice of representation. One choice has been the fermionic representations of SU($N$), where the $N=\infty$ ground state is constructed by dimerizing all spins into near-neighbor singlet pairs. To select among the many dimerizations, $1/N$ corrections must be computed. This is where the *kagomé* structure first enters the picture. Considering only the lowest nonvanishing corrections, Marston and Zeng[8] found that the preferred dimer configurations have the maximum number of hexagons covered by three dimers. This still leaves a large degeneracy; in particular, the state having three dimers at one hexagon rotated by 60° has the same energy. Sachdev,[4] using bosonic representations for the groups Sp($N$), finds a low-spin phase of the *kagomé* antiferromagnet where no symmetries (including spin) are broken. This is in conflict with the SU($N$) prediction where translational symmetry—in the form of near-neighbor spin-spin expectation values—is broken.

The approach used in this paper is similar in spirit to the "quantum dimer model" introduced by Kivelson and Rokhsar[9,10] for the square lattice spin-$\frac{1}{2}$ antiferromagnet. In this model the Hilbert space is spanned by the same kinds of states that are selected at large $N$ for the SU($N$) model. However, since $N$ is kept equal to 2, the tunneling amplitude between different dimerizations is not an exponentially small quantity and the ground state takes the form of a superposition. There are two difficulties with this approach: the enumeration of the dimer basis states, and the nonorthogonality of the basis. For the *kagomé* structure it was shown[3] that the entropy of dimer coverings is equal to $(N/3)\ln 2$ where $N$ is the number of spins. Since $N/3=M$ is just the number of hexagons, this suggests it is possible to represent dimer states by Ising variables associated with the hexagons in the structure. Moreover, as was already hinted by Kivelson and Rokhsar,[9] it should be possible to develop an expansion of matrix elements by taking advantage of their exponential decay with the length of loops appearing in the corresponding transition graph (superposition of the two dimerizations). The *kagomé* structure is an excellent candidate for this type of expansion, since the shortest nontrivial transition graph must contain a loop of length 6 that surrounds one hexagon. The small parameter in the expansion can be made explicit by considering a generalization of the *kagomé* structure, where each hexagon is replaced by a polygon of $n$ sides and treating $n$ as large. For $n>6$, such structures are homogeneous when embedded in the hyperbolic plane with curvature becoming more negative as $n$ increases. Thus we may think of the limit $n\to\infty$ as joining the more familiar geometrical device $d$(dimensionality)$\to\infty$ in the elucidation of interacting lattice systems.

We wish to stress that our use of negative curvature is

 

strictly formal. Although the method has identified a new small parameter in a class of models, in the end we will *only* be interested in the case $n=6$. Generalized *kagomé* structures with $n>6$ are pathological in having an extensive boundary. There are serious problems in properly defining, for example, the asymptotics of correlation functions on such objects and we do not attempt to do so. Our interest in the curvature expansion method is confined to the derivation (order by order) of an effective Hamiltonian. Once obtained, this Hamiltonian will only be used for the original zero-curvature *kagomé* model.

The body of this paper is organized as follows. Section II describes the pseudospin representation of the dimer states and gives formulas for overlap and Hamiltonian matrix elements in the $n\to\infty$ limit. In Sec. III the form of the ground-state wave function—including next-nearest-neighbor singlet-bond fluctuations—is specified and an effective Hamiltonian for the pseudospins is derived. Using coherent-state wave functions for the pseudospins, the energies of various schemes of translational symmetry breaking are investigated. Conclusions are given in Sec. IV.

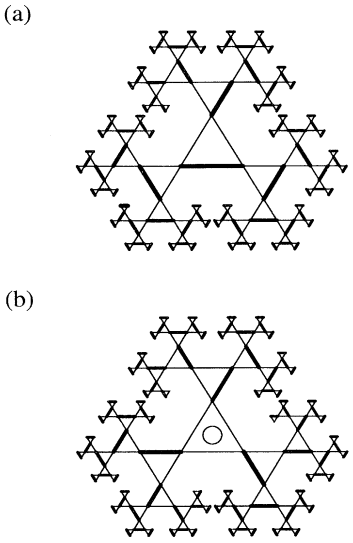


FIG. 1. Generalized *kagomé* structure in the $n=\infty$ limit. (a) Dimerization with no defects. (b) Dimerization with one defect (indicated by circle).

## II. DIMERIZED STATES IN THE HYPERBOLIC PLANE

### A. Pseudospin representation

We choose the additive constant in the definition of the Hamiltonian so that for $n=\infty$, the ground-state energy is zero:

$$\mathcal{H}=\sum_{(ij)}(\mathbf{S}_i\cdot\mathbf{S}_j+\tfrac{1}{4})=\sum_{(ijk)}H_{ijk}\ , \tag{2.1}$$

where

$$H_{ijk}=\tfrac{1}{2}(\mathbf{S}_i+\mathbf{S}_j+\mathbf{S}_k)^2-\tfrac{3}{8} \tag{2.2}$$

is the interaction among spins on one triangle of the *kagomé* structure. In what follows, the notations $(ij)$ and $(ijk)$ denote nearest-neighbor and three mutually nearest-neighbor objects, respectively. For $n=\infty$, the assembly of triangles forms no closed loops and the structure becomes the tree shown in Fig. 1. Moreover, one can then dimerize the spins [Fig. 1(a)] so that each triangle contains one singlet pair and becomes a spin-$\frac{1}{2}$ object. Because $H_{ijk}$ is linearly related to the total spin operator on a triangle—with the lowest eigenvalue corresponding to total spin-$\frac{1}{2}$—we see that constructions such as shown in Fig. 1 give the lowest possible energy for the whole system (zero).

There are other dimerizations where some triangles contain no singlet bonds. Such triangles represent defects in the dimerization because they have positive energy; an example is shown in Fig. 1(b). Dimerizations containing defects are no longer eigenstates of the Hamiltonian (2.1) but this can be fixed by including singlet-bond fluctuations (next-nearest neighbor, etc.) localized around the defect.[3] A useful property of defects is that we may view their number $N_d$ as being conserved. This comes about rather trivially for the case $n=\infty$, in that the transition graph of two distinct dimerizations contains an infinite chain of singlets, thus causing all off-diagonal matrix elements to vanish. For finite $n$, loops in the transition graph can move defects around but their number will not change. To see this it is convenient to represent dimerizations by means of arrows on the edges of a graph composed of only $n$-sided polygons. Figure 2 shows an arrow pattern for a structure formed out of 7-sided polygons in the hyperbolic plane. The allowed combinations of arrows at each vertex correspond to the two types of triangle dimerizations shown in Fig. 3. Arrow patterns of two different dimerizations are related by reversing arrows on simple closed paths since at each vertex either zero or two arrows must be reversed in order to remain consistent with the vertex rules. The pattern of arrow reversals is, in fact, just another representation of the transition graph. Now, if two dimerizations have a nonvanishing matrix element, the length of their transition graph must be finite so that the corresponding arrow reversals occupy a finite region. The directions of arrows crossing the boundary of this region and, in particular, their flux

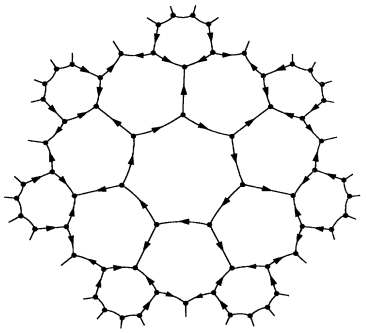

FIG. 2. Tiling of the hyperbolic plane by 7-sided polygons. The arrangements of arrows at each vertex corresponds to one of the two triangle dimerization in Fig. 3.

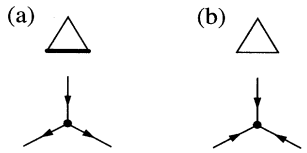


FIG. 3. Representation of triangle dimerizations by arrows. The flux of arrows from a triangle with a defect (b) is $(-3)$ times the flux from a triangle without a defect (a).

must be the same for the two states. But because the flux of arrows crossing the boundary is just the sum of the net divergence of arrows at each triangle, which is different for defect and nondefect triangles, the number of enclosed defects cannot change.

That defects are unavoidable when $n$ is finite can be seen from trying to dimerize spins on triangles belonging to just two adjacent polygons. For the ordinary *kagomé* structure, i.e., $n=6$, the boundary of a large, compact (e.g., circular) region is crossed by far fewer arrows than vertices enclosed by it. Thus the average divergence of arrows at each vertex is required to be zero, giving a defect fraction of $\frac{1}{4}$ (Ref. 3). This is no longer true for $n>6$, where the length of boundary grows as fast as the enclosed number of vertices and a nonvanishing mean divergence can be accommodated.

Since any two dimerized states are related by loops of arrow reversals on an arrow diagram (Fig. 2), the set of all dimerized states can be enumerated by fixing one dimerized state as a reference state $|D_0\rangle$ and specifying all other states in terms of appropriate arrow reversals. Moreover, the possible patterns of arrow reversals correspond essentially to the set of all Ising domain walls generated in a model where a pseudospin $\sigma^z=\pm 1$ is situated at each polygon center. To help us distinguish the pseudospin states from the states of the original spin model, we will use the notation

$$||D\rangle\rangle=||\sigma_1^z,\ldots,\sigma_M^z;D_0\rangle\rangle\ , \tag{2.3}$$

where $D_0$ represents the reference dimerization. Clearly a pseudospin state with all $\sigma^z$ values reversed corresponds to the same domain-wall pattern and the same physical state. This twofold global redundancy should not affect properties of the model in the thermodynamic limit. In a finite system with periodic boundary conditions (realizable for $n=6$) it is possible for two dimerizations to be related by a transition graph with odd winding numbers around the torus—thus making a two-coloring of Ising domains impossible.[11] This topological relationship between dimerizations decomposes the set of states into four equivalent sectors, each of which can be represented in the form (2.3). In a large enough system it is not necessary to consider the mixing of states from different sectors since the corresponding matrix elements are exponentially small.

### B. Matrix elements

In the hyperbolic plane, the domain wall around a cluster of flipped pseudospins grows in proportion to the number of enclosed pseudospins. Since overlap matrix elements of dimerized states decay exponentially with the length of the boundary, they also decay exponentially in the number of overturned pseudospins. For the lowest nontrivial order in an approximate calculation, we consider only a single flipped pseudospin. Specifically, we are interested in dimerized states $|D\rangle$ and $|D'\rangle$ with the pseudospin representations,

$$||D\rangle\rangle=||\sigma_1^z,\ldots,\sigma_r^z,\ldots,\sigma_M^z\ ;D_0\rangle\rangle\ , \tag{2.4a}$$

$$||D'\rangle\rangle=||\sigma_1^z,\ldots,-\sigma_r^z,\ldots,\sigma_M^z\ ;D_0\rangle\rangle\ . \tag{2.4b}$$

The matrix element $\langle D|D'\rangle$ depends on our convention for the orientations of the singlet wave functions, i.e., the order of spin up and down along the bond that produces a positive sign. The simplest choice for general $n$ is to orient the singlets clockwise around the triangles. With this choice we obtain

$$\langle D|D'\rangle=\langle\langle D||\sigma_r^x f_r||D'\rangle\rangle=O(\epsilon)\ , \tag{2.5}$$

where

$$f_r=2(-\tfrac{1}{2})^{n/2}\prod_{(pqr)}(z+z^*\sigma_p^z\sigma_q^z) \tag{2.6}$$

is a product of $n$ factors involving the pseudospins which surround pseudospin $r$, and $z=\frac{1}{2}+i/\sqrt{8}$. The formula for $f_r$ depends on the reference state $D_0$. The choice of $D_0$ used in (2.6) is the one (valid for even $n$) where dimers alternate around the polygon of the flipped pseudospin as shown for $n=6$ in Fig. 4(a). Other choices of $D_0$ correspond to replacing some combination of the $\sigma^z$ in (2.6) by their negatives. An example is shown in Fig. 4(b), where the correct formula is given by the substitution $\sigma_1^z\rightarrow-\sigma_1^z$. For $n=6$, the value of $f_r$ varies from $-\frac{1}{4}$, when the transition graph is a hexagon, to $\frac{1}{32}$, when the transition graph is a six-pointed star. We will use $\epsilon=2^{1-n/2}$—the largest absolute value of the overlap—to denote the small parameter in our expansion.

Diagonal matrix elements of the Hamiltonian merely count the number of defects in the dimerization,[3] i.e.,

$$\langle D|\mathcal{H}|D\rangle=\Delta N_d\ , \tag{2.7}$$

where $\Delta=\frac{3}{4}$ is the energy of one defect. Off-diagonal elements involving one flipped pseudospin are given by the formula

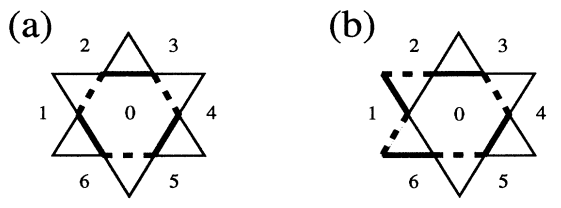


FIG. 4. Reference dimerization $D_0$ used in the definition of matrix elements. Case (a) corresponds to formulas (2.6) and (2.9); (b) corresponds to replacing $\sigma_1^z$ in these formulas by $-\sigma_1^z$. Broken bonds show the dimerization when the sign of the central pseudospin ($\sigma_0^z$) has been reversed.

$$\langle D|\mathcal{H}|D'\rangle = \Delta \langle\langle D||\sigma_r^x f_r (N_d - g_r)||D'\rangle\rangle = O(\epsilon) , \quad (2.8)$$

where

$$g_r = \frac{1}{4} \sum_{(pqr)} (\sigma_p^z \sigma_q^z + 1) . \quad (2.9)$$

The remarks concerning the choice of reference dimerization given above apply here as well. For a different choice, appropriate combinations of $\sigma^z$ are replaced by their negatives in both $f_r$ and $g_r$.

## III. GROUND-STATE WAVE FUNCTIONS

### A. Defect fluctuations

As discussed above, at finite $n$ all dimerizations have a nonvanishing density of defects. When the Hamiltonian acts on a state containing defects, the resulting state has an admixture of next-nearest-neighbor singlet bonds in the vicinity of each defect. A good variational wave function must include such fluctuations in each of the dimerized states of the superposition. We will consider the simple one-parameter class of wave functions formed by superimposing

$$|D_\alpha\rangle = \prod_{\substack{\text{defects in } D \\ (ijk)}} (1 + \alpha H_{ijk}) |D\rangle , \quad (3.1)$$

where the $N_d$ factors in the product commute since defects never occur on neighboring triangles. Wave function (3.1) does quite well on the $n = \infty$ tree when the dimerization contains one defect [Fig. 1(b)]. There, one obtains the Hamiltonian expectation value

$$\Delta_\alpha = \frac{3/4 + (9/4)\alpha + (45/16)\alpha^2}{1 + (3/2)\alpha + (9/8)\alpha^2} . \quad (3.2)$$

The minimum, $\Delta_\alpha = \frac{1}{2}$ is achieved for $\alpha = -\frac{1}{3}$ and represents a significant improvement over the "bare" defect energy $\Delta_0 = \frac{3}{4}$. Including higher-order fluctuations around the defect does not improve the energy greatly. At the next order, incorporating up to two applications of $\mathcal{H}$ in the admixture, the energy is only reduced to 0.4708. When there are more defects on the tree structure, one finds

$$\frac{\langle D_\alpha|\mathcal{H}|D_\alpha\rangle}{\langle D_\alpha|D_\alpha\rangle} = \Delta_\alpha N_d + O(\alpha^4) , \quad (3.3)$$

where the first term is independent of the defect arrangement. Thus, at the level of defect fluctuations of the form (3.1), it appears that defects are noninteracting. This is no longer true at finite $n$, although the interactions turn out to be extremely small (see Sec. III B).

### B. Pseudospin Hamiltonian

Perhaps a more important improvement of the wave function for finite $n$ (in particular, $n = 6$) is to form a superposition of dimerizations $D$:

$$|\psi_\alpha\rangle = \sum_D \psi(D) |D_\alpha\rangle . \quad (3.4)$$

A pseudospin state can be defined which uses the same amplitudes:

$$||\psi\rangle\rangle = \sum_D \psi(D) ||D\rangle\rangle . \quad (3.5)$$

The main advantage of (3.5) is the orthogonality of the basis states $||D\rangle\rangle$. The norm of (3.4), when expressed in terms of (3.5), is given by the expectation value of an operator that is off diagonal in the pseudospins. An expansion of this operator in powers of $\epsilon$ resembles a Mayer cluster expansion. The first term in the expansion is order $\epsilon^0$. This is followed by $M$ terms of order $\epsilon^1$, $M^2$ terms of order $\epsilon^2$, etc. The $M^2$ terms of order $\epsilon^2$ are, of course, just half the square of the first-order terms plus $O(M)$ additional terms of order $\epsilon^2$. By the usual linked cluster theorem, the expansion exponentiates giving

$$\langle\psi_\alpha|\psi_\alpha\rangle = \langle\langle\psi||\exp(S_\alpha)||\psi\rangle\rangle = \langle\langle\phi||\phi\rangle\rangle , \quad (3.6)$$

where

$$||\phi\rangle\rangle = \exp(\tfrac{1}{2}S_\alpha)||\psi\rangle\rangle . \quad (3.7)$$

For $\alpha = 0$, we can use the formulas in Sec. II B to obtain

$$S_0 = \sum_{r=1}^{M} \sigma_r^x f_r + O(\epsilon^2) . \quad (3.8)$$

The effective pseudospin Hamiltonian $\mathcal{H}_\alpha$ is defined by

$$\frac{\langle\langle\phi||\mathcal{H}_\alpha||\phi\rangle\rangle}{\langle\langle\phi||\phi\rangle\rangle} = \frac{\langle\psi_\alpha|\mathcal{H}|\psi_\alpha\rangle}{\langle\psi_\alpha|\psi_\alpha\rangle} . \quad (3.9)$$

The denominators in (3.9) are equal so that we need to construct the operator $\mathcal{H}_\alpha$ with the property that

$$\langle\langle\psi||\exp(\tfrac{1}{2}S_\alpha)\mathcal{H}_\alpha\exp(\tfrac{1}{2}S_\alpha)||\psi\rangle\rangle = \langle\psi_\alpha|\mathcal{H}|\psi_\alpha\rangle \quad (3.10)$$

for arbitrary amplitudes $\psi(D)$. Again, using a cluster expansion in powers of $\epsilon$ to evaluate the right-hand side of (3.10) and expanding $\exp(\frac{1}{2}S_\alpha)$ in powers of $\epsilon$ as well, we obtain

$$\mathcal{H}_\alpha = \Delta_\alpha N_d + \mathcal{H}_\alpha^1 + O(\epsilon^2) . \quad (3.11)$$

The formulas in Sec. II B are sufficient to evaluate the $\epsilon^1$ term for $\alpha = 0$:

$$\mathcal{H}_0^1 = -\Delta_0 \sum_{r=1}^{M} \sigma_r^x f_r g_r + O(\epsilon^2) . \quad (3.12)$$

When multiplied out for the ordinary *kagomé* structure ($n = 6$), the coefficient of $\sigma_0^x$ is given by

$$\begin{aligned} f_0 g_0 = {} & c_1 + c_2(\sigma_1^z\sigma_2^z + \cdots) + c_3(\sigma_1^z\sigma_3^z + \cdots) \\ & + c_4(\sigma_1^z\sigma_4^z + \cdots) + c_5(\sigma_1^z\sigma_2^z\sigma_3^z\sigma_4^z + \cdots) \\ & + c_6(\sigma_1^z\sigma_2^z\sigma_3^z\sigma_5^z + \cdots) + c_7(\sigma_1^z\sigma_2^z\sigma_4^z\sigma_5^z + \cdots) \\ & + c_8\sigma_1^z\sigma_2^z\sigma_3^z\sigma_4^z\sigma_5^z\sigma_6^z . \end{aligned} \quad (3.13)$$

The reference state $D_0$ as well as the numbering scheme for pseudospins shown in Fig. 4(a) has been used. Terms indicated by $\cdots$ in (3.13) are cyclic permutations of the leading term and the coefficients have values

$$(c_1,\ldots,c_8) = \tfrac{1}{512}(33,13,-15,-27,-15,-27,-15,-27) . \quad (3.14)$$

When $\alpha\neq 0$, the expression for $\mathcal{H}^1_\alpha$ changes in three ways: (a) the coefficients $(c_1,\ldots,c_8)$ become functions of $\alpha$ (as does the defect energy, $\Delta_\alpha$); (b) new diagonal terms (involving only $\sigma^z$) appear; and (c) new off-diagonal terms appear which couple $\sigma^x$ at one site with $\sigma^z$ at next-nearest-neighbor sites. Both (b) and (c) are of order $\epsilon^1$ but unlike (a) they vanish as $\alpha^2$ for small $\alpha$. Terms (b) and (c) were also found to be numerically very small in the case of interest ($n=6$, $\alpha\approx-\frac{1}{3}$) and were neglected in the calculations described in the next section. The coefficient functions for $n=6$ are tabulated in the Appendix.

We note that once a state is constructed from a superposition of dimerized states, it is no longer obvious that the spin-spin correlations are short ranged. It was shown by Kohmoto and Shapir[12] that this property is preserved on the square lattice even when all dimerized states are given equal amplitude. We fully expect this to be the case on the *kagomé* structure as well.

### C. Pseudospin coherent states

Finding the ground state of the pseudospin Hamiltonian $\mathcal{H}_\alpha$ to order $\epsilon^1$ is clearly the same as finding the ground state of the operator $\mathcal{H}^1_\alpha$. Since the latter describes resonance among dimerized states, we refer to its lowest eigenvalue as the resonance energy. We note however that $\mathcal{H}^1_\alpha$ is quite nontrivial, certainly no simpler than the original *kagomé* Hamiltonian. This should not be viewed as a failure of the present enterprise but rather as the unavoidable result of having exposed the low-energy degrees of freedom in the original model. With this in mind we expect that even a relatively crude treatment of the $\mathcal{H}^1_\alpha$ ground state should shed some interesting light on the problem.

A simple upper bound on the resonance energy can be found using coherent-state wave functions for the pseudospins:

$$||\phi\rangle\rangle = ||\sigma_1\rangle\rangle\otimes\cdots\otimes||\sigma_M\rangle\rangle . \quad (3.15)$$

Taking the expectation value of $\mathcal{H}^1_\alpha$ in (3.15) simply replaces the pseudospin operators $\boldsymbol{\sigma}$ by unit vectors. The coherent state with all unit vectors parallel or antiparallel to the $z$ axis corresponds to a definite dimerized state and has zero resonance energy, i.e., $\langle\langle\mathcal{H}^1_\alpha\rangle\rangle=0$. Resonance always lowers the energy. It is easily seen that in the optimal arrangement all the unit vectors lie in the $x$-$z$ plane. Consider rotating a particular unit vector $\mathbf{n}_0$ about the $z$ axis. The only change in $\langle\langle\mathcal{H}^1_\alpha\rangle\rangle$ produced by this rotation is the change in the single term which depends on $n^x_0$. Since $n^x_0$ appears linearly, a suitable rotation will make this term negative (or zero) and at the optimal rotation angle $n^y_0=0$. We may, therefore, assume that in the ground state each unit vector is specified by a single "resonance" angle $\theta$ where $(n^x,n^z)=(\cos\theta,\sin\theta)$.

The state formed by taking an equal amplitude superposition of all dimerized states (with fluctuations added around defects) corresponds to the choice $\theta=0$ for all pseudospins. From (3.12) we see that the resonance energy per pseudospin on the ordinary *kagomé* structure is just $-c_1\Delta_\alpha$ in (3.13); its behavior with $\alpha$ is shown by the upper curve in Fig. 5. This maximally resonant state is translationally invariant and has been called a "spin liquid."

By breaking translational symmetry, the resonance energy can be lowered further. This comes about through the "order by disorder" mechanism already noticed by Sachdev[10] in the simple square lattice quantum dimer model.[9] Three periodic patterns of translational symmetry breaking for the *kagomé* structure are shown in Fig. 6. The reference state $D_0$ is indicated in each diagram by the thick unbroken bonds. It is a relatively straightforward numerical exercise to find the angles $\theta_A,\theta_B,\ldots,$ which minimize the resonance energy in each case. This was done for $-0.6<\alpha<0$; the results are given as the three lower curves in Fig. 5. Pattern (a) in Fig. 6 has the smallest unit cell which has the full point-group symmetry. At the resonance angles $\theta_A=\theta_B=\pi/2$ the defects (indicated by circles) are arranged in the honeycomb pattern of the reference state. The energy per defect, i.e.,

$$\epsilon_d=\Delta_\alpha+\langle\langle\mathcal{H}^1_\alpha\rangle\rangle/N_d , \quad (3.16)$$

is minimized for $\alpha=-0.327$ and $\theta_A=34.5°$, $\theta_B=82.7°$. Since $|\cos\theta_B|$ is relatively small, the resonance energy is dominated by the $A$ pseudospins. The most important off-diagonal matrix elements correspond to parallelogram shaped transition graphs around the $A$ pseudospins. For this matrix element $f_A=+\frac{1}{8}$, which explains why the optimal $\theta_A$ is close to zero rather than $\pi$.

A significant further lowering of the energy is achieved in patterns such as 6(b) and 6(c) where the defects are condensed into resonating six-pointed stars.[3] Pattern (b) is the smallest unit cell with this property; pattern (c) is the smallest which has the full point-group symmetry. The reference states in these patterns are essentially the same as those identified by the SU($N$) analysis of Marston and Zeng.[8] The minimum of $\epsilon_d$ for both patterns occurs

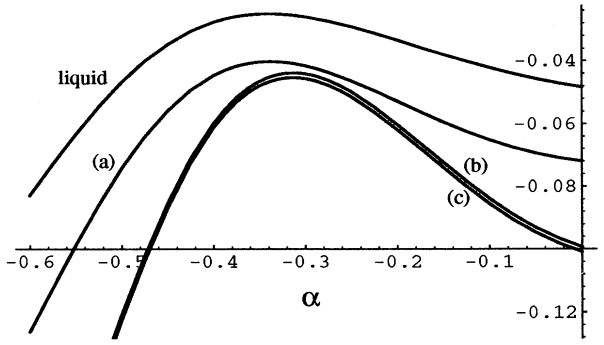


FIG. 5. Resonance energy $\langle\langle\mathcal{H}^1_\alpha\rangle\rangle$ per pseudospin of four coherent-state wave functions as a function of $\alpha$. Upper curve is the liquid; remaining curves, from top to bottom, correspond to symmetry-breaking patterns (a), (b), and (c) in Fig. 6.

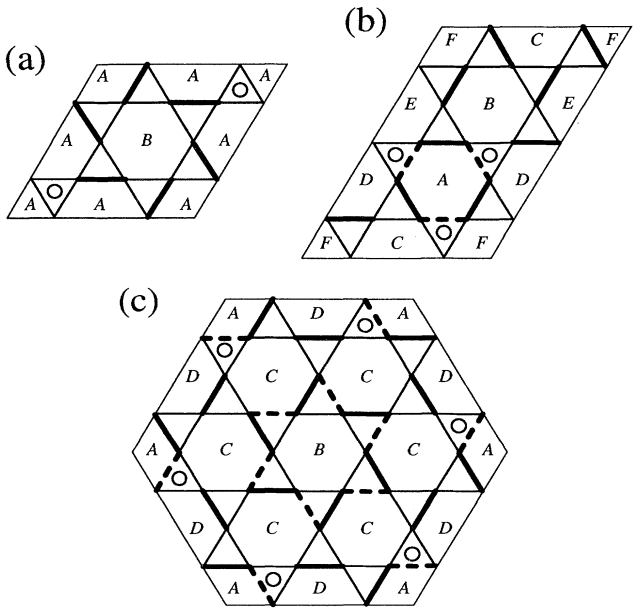


FIG. 6. Three translational symmetry-breaking patterns. Hexagons bearing the same label ( $A$, $B$, etc.) have the same resonance angle $\theta$. The dimerization corresponding to $\theta_A=\theta_B=\cdots=\pi/2$ is represented by thick unbroken bonds. Optimal resonance angle for hexagon $A$ in (b) and hexagons $A$ and $B$ in (c) is $\pi$ and corresponds to an equal amplitude superposition of the broken and unbroken bond dimerizations. The number of *kagomé* spins per unit cell in (a), (b), and (c) is 12, 18, and 36, respectively.

when the resonance angle of particular pseudospins, labeled $A$ in the figure, is $\pi$. This maximal form of resonance is distinct from the situation in pattern (a) (where $\theta_A$ is closer to zero) and is explained by the fact that $f_A=-\frac{1}{4}$ is negative for the short hexagonal transition graph generated by flipping one of these pseudospins. In the more symmetrical pattern (c), the angle $\theta_B$ is also $\pi$ at the minimum but the contribution to the resonance energy from this hexagon is actually quite small. Over the range of $\alpha$ considered, the resonance energy of pattern (c) (lower curve in Fig. 5) was always slightly lower than that of (b). The lowest energy, $\varepsilon_d=0.3723$, was achieved for $\alpha=-0.510$ and $\theta_C=97.1°$, $\theta_D=78.1°$. To express this energy in the more conventional terms of energy per spin for the Hamiltonian without the additive constant $\frac{1}{4}$, we use the formula $\varepsilon_{\text{conv}}=(\varepsilon_d-3)/6=-0.4380$. This compares well with the value $\varepsilon_{\text{conv}}=-0.4384$ obtained by numerical diagonalization of a 36-site *kagomé* cluster.[7]

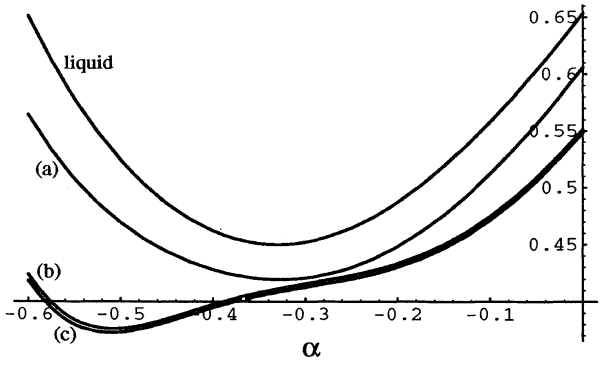


FIG. 7. Energy per defect $\varepsilon_d=\Delta_\alpha+\langle\langle\mathcal{H}_\alpha^1\rangle\rangle/N_d$ corresponding to the four curves in Fig. 5.

Figure 7 shows $\varepsilon_d$ for the spin-liquid and the three-symmetry broken states (Fig. 6) as a function of $\alpha$. The behavior of all the curves is dominated by the function $\Delta_\alpha$ which has a minimum at $\alpha=-\frac{1}{3}$. Thus, most of the lowering of the energy comes from the inclusion of defect fluctuations. In contrast, energy differences between different resonance patterns are generally quite small, particularly so for patterns such as (b) and (c) (Fig. 6), where defects have condensed onto the smallest possible number of stars. Resonance effects would be even smaller in hyperbolic geometries with $n>6$ while the magnitude of defect fluctuations would remain the same.

## IV. CONCLUSIONS

Strong numerical evidence ruling out long-range spin order in the spin-$\frac{1}{2}$ *kagomé* antiferromagnet[6,7] suggests that a good ground-state wave function can be constructed using short-range singlet pairs or dimers. The large degeneracy in the energy of dimerized states is removed by resonance. A means for studying this kind of ground-state selection is provided by an effective Hamiltonian which acts on pseudospins situated in the hexagons of the *kagomé* structure. A systematic derivation of the pseudospin Hamiltonian is made possible by considering generalizations of the *kagomé* structure in the hyperbolic plane.

The picture of the ground state that has emerged from this approach is consistent with an earlier study[3] but is more detailed in some respects. Resonance is concentrated at a minority of the hexagons in the structure—the same hexagons where there is a large probability of finding defects in the dimerization. In the coherent-state approximation, the pseudospin Hamiltonian predicts a particular arrangement of such hexagons [Fig. 6(c)] in the ground state. Alternative arrangements, however, have only slightly higher energy, creating the suspicion that higher-order corrections to the pseudospin Hamiltonian or defect fluctuations might need to be included to reliably resolve these differences. It may also be the case that quantum fluctuations in the treatment of the pseudospin Hamiltonian are important in a qualitative way. Thus, tunneling among the quasidegenerate arrangements of minority hexagons could restore translational symmetry. It is not obvious how small the diagonal energy shifts of the different arrangements would have to be in order for tunneling to play a role, since the tunneling amplitudes for such large scale rearrangements would themselves be extremely small. Irrespective of whether the solid or liquid prevails in the end, we can be sure that the energy scale of excitations within the singlet sector is extremely small.

## ACKNOWLEDGMENTS

Part of the work described in this paper was carried out at the Institute for Theoretical Physics in Santa Barbara and was supported in part by the National Science Foundation under Grant No. PHY89-04035. Additional support was provided by the David and Lucille Packard Foundation. We thank Chris Henley for his useful criticisms on an early version of this paper.


## APPENDIX

There are eight symmetry inequivalent transition graphs possible when a single pseudospin is flipped; two are shown in Fig. 4. These involve as few as zero and as many as six defects and corresponding fluctuation factors $(1+\alpha H_{ijk})$ in the initial and final states combined. Overlap and Hamiltonian matrix elements are, therefore, polynomials of degree 6 in $\alpha$; they were evaluated by a FORTRAN computer program. The basic matrix elements were manipulated by *Mathematica* to give the coefficients $c_1,\ldots,c_8$. When expressed in terms of a common denominator,

$$q=128(8+12\alpha+9\alpha^2)^3(4+12\alpha+15\alpha^2)\ , \tag{A1}$$

the coefficients have the form $c_i=p_i/q$ where the $p_i$ are polynomials in $\alpha$ of degree 8:

$$p_1=16\,896+116\,736\alpha+331\,392\alpha^2+460\,608\alpha^3+296\,328\alpha^4-25\,368\alpha^5-144\,702\alpha^6-61\,128\alpha^7-6993\alpha^8\ , \tag{A2}$$

$$p_2=6656+45\,056\alpha+149\,120\alpha^2+297\,024\alpha^3+358\,056\alpha^4+229\,512\alpha^5+63\,882\alpha^6+1944\alpha^7-1485\alpha^8\ , \tag{A3}$$

$$p_3=-7680-51\,200\alpha-116\,608\alpha^2-59\,072\alpha^3+134\,280\alpha^4+231\,528\alpha^5+152\,010\alpha^6+48\,600\alpha^7+6777\alpha^8\ , \tag{A4}$$

$$p_4=-13\,824-86\,016\alpha-191\,872\alpha^2-103\,872\alpha^3+217\,960\alpha^4+423\,240\alpha^5+317\,754\alpha^6+118\,152\alpha^7+18\,279\alpha^8\ , \tag{A5}$$

$$p_5=-7680-55\,296\alpha-142\,720\alpha^2-122\,048\alpha^3+57\,352\alpha^4+181\,608\alpha^5+138\,834\alpha^6+49\,032\alpha^7+7263\alpha^8\ , \tag{A6}$$

$$p_6=-13\,824-98\,304\alpha-278\,400\alpha^2-365\,504\alpha^3-226\,072\alpha^4-39\,096\alpha^5+22\,482\alpha^6+11\,016\alpha^7+1269\alpha^8\ , \tag{A7}$$

$$p_7=-7680-55\,296\alpha-157\,056\alpha^2-200\,896\alpha^3-127\,736\alpha^4-58\,008\alpha^5-43\,470\alpha^6-27\,432\alpha^7-7317\alpha^8\ , \tag{A8}$$

$$p_8=-13\,824-110\,592\alpha-344\,448\alpha^2-506\,304\alpha^3-382\,872\alpha^4-132\,792\alpha^5-1494\alpha^6+10\,152\alpha^7+1755\alpha^8\ . \tag{A9}$$


[1] C. Broholm, G. Aeppli, G. P. Espinosa, and A. S. Cooper, Phys. Rev. Lett. **65**, 3173 (1990).
[2] D. S. Greywall, Phys. Rev. B **41**, 1842 (1990).
[3] V. Elser, Phys. Rev. Lett. **62**, 2405 (1990).
[4] S. Sachdev, Phys. Rev. B **45**, 12 377 (1992).
[5] A. Chubukov (unpublished).
[6] R. R. P. Singh and D. A. Huse, Phys. Rev. Lett. **68**, 1766 (1992).
[7] P. W. Leung and V. Elser, Phys. Rev. B **47**, 5459 (1993).
[8] J. B. Marston and C. Zeng, J. Appl. Phys. **69**, 5962 (1991).
[9] D. Rokhsar and S. Kivelson, Phys. Rev. Lett. **61**, 2376 (1988).
[10] S. Sachdev, Phys. Rev. B **40**, 5204 (1989).
[11] N. Read and B. Chakraborty, Phys. Rev. B **40**, 7133 (1989).
[12] M. Kohmoto and Y. Shapir, Phys. Rev. B **37**, 9439 (1988).